

Short communication

## Discharge properties of all-solid sodium–sulfur battery using poly (ethylene oxide) electrolyte

Cheol-Wan Park<sup>a</sup>, Ho-Suk Ryu<sup>b</sup>, Ki-Won Kim<sup>b,c</sup>, Jou-Hyeon Ahn<sup>d</sup>,  
Jai-Young Lee<sup>e</sup>, Hyo-Jun Ahn<sup>b,c,\*</sup>

<sup>a</sup> SODIFF Advanced Materials Company, Yeongju, South Korea

<sup>b</sup> Global Leader Development Center for I-cube Materials and Parts, Gyeongsang National University, Jinju, South Korea

<sup>c</sup> School of Nano and Advanced Materials Engineering, Gyeongsang National University, Jinju, South Korea

<sup>d</sup> Department of Chemical & Biological Engineering, Gyeongsang National University, Jinju, South Korea

<sup>e</sup> Department of Fusion Technology, Konkuk University, Seoul, South Korea

Received 12 September 2006; accepted 24 November 2006

Available online 16 January 2007

### Abstract

An all-solid sodium/sulfur battery using poly (ethylene oxide) (PEO) polymer electrolyte are prepared and tested at 90 °C. Each battery is composed of a solid sulfur electrode, a sodium metal electrode, and a solid PEO polymer electrolyte. During the first discharge, the battery shows plateau potentials at 2.27 and at 1.76 V. The first discharge capacity is 505 mAh g<sup>-1</sup> sulfur at 90 °C. The capacity drastically decreases by repeated on charge–discharge cycling but remains at 166 mAh g<sup>-1</sup> sulfur after 10 cycles. The latter value is higher than that reported for a Na/poly (vinylidene difluoride)/S battery at room temperature.

© 2006 Elsevier B.V. All rights reserved.

**Keywords:** Sodium battery; Sulfur electrode; Poly (ethylene oxide) polymer electrolyte; Solid-state battery; Capacity; Charge-discharge cycling

### 1. Introduction

The application of batteries in portable electronic devices and electric vehicles has rapidly expanded [1,2]. Many researchers have attempted to obtain a battery that has high specific energy density, high specific power and low material cost [3,4]. In particular sodium–sulfur, (Na–S) battery systems have been studied extensively because of their low material cost, long cycle-life, and high specific energy [5]. Kummer and Weber [6] reported the electrochemical properties of a Na/S battery above 300 °C. The Na/S battery could operate at this temperature because the β"-alumina ceramic electrolyte showed high sodium ionic conductivity. At the high operating temperature, sodium (mp = 97.8 °C) and sulfur (mp = 110 °C) melted into liquid states that were more reactive and corrosive than the solid states. On the other hand, liquid sodium and sulfur could induce explo-

sions and corrosion, and power was consumed in maintaining the operating temperature [2].

Extensive research has been performed to improve high-temperature Na/S batteries [5–9]. In order to develop solid-state Na/S batteries, the electrolyte should have high ionic conductivity below the melting temperatures of sodium and sulfur. All-solid batteries based on polymer electrolytes appear to be ideal power sources for electric vehicles (EVs) and hybrid electric vehicles (HEVs) due to their safety and feasible designs [10]. Polymer electrolytes are attractive in that they can lead to flexible, compact and safe all-solid batteries [11]. Several types of polymer have been studied as sodium-ion conducting electrolytes at low temperatures [12–17]. Poly (ethylene oxide) (PEO) and ‘glymes’ (CH<sub>3</sub>O(CH<sub>2</sub>CH<sub>2</sub>O)<sub>n</sub>CH<sub>3</sub>), were found to be compatible with the sulfur electrode [18–20]. Abraham and Jiang [21] have investigated poly (vinylidene fluoride-hexa fluoropropene) (PVdF-HFP) copolymer with poly (ethylene glycol) dimethylether (PEGDME). Park et al. [17] reported that a room-temperature Na/S battery using a gel polymer electrolyte gave a high discharge capacity of 489 mAh g<sup>-1</sup> sulfur.

\* Corresponding author. Tel.: +82 55 751 5308; fax: +82 55 759 1745.  
E-mail address: [ahj@gnu.ac.kr](mailto:ahj@gnu.ac.kr) (H.-J. Ahn).

Poly (ethylene oxide) is a very stable solid polymer electrolyte that has high ionic conductivity at a moderately high temperature [18,19]. There have been investigations of PEO with sodium trifluoromethane sulfonate ( $\text{NaCF}_3\text{SO}_3$ ) [14] and sodium nitrate ( $\text{NaNO}_3$ ) [13], but no studies of an all-solid Na/S battery using a PEO electrolyte. Accordingly, this paper reports the electrochemical properties of a Na/S battery with a PEO polymer electrolyte that is operated at 90 °C.

## 2. Experiment

In order to remove water from the raw materials, elemental sulfur powder and PEO (average mass  $M_w = 4 \times 10^6$ , Aldrich) were dried under vacuum at 60 °C for 24 h. Carbon and  $\text{NaCF}_3\text{SO}_3$  were dried under vacuum at 90 °C for 24 h. A sulfur electrode was prepared from a suspension of 70 wt.% elemental sulfur powder, 20 wt.% carbon and 10 wt.% PEO in acetonitrile. The suspension was mixed for 2 h in an attrition ball mill and then cast on to a glass dish. The sulfur electrode films were heated at 60 °C for 24 h in a vacuum. The sodium electrode was prepared by cutting a sodium ingot in an argon atmosphere.

The PEO polymer electrolyte was prepared by dissolving PEO and  $\text{NaCF}_3\text{SO}_3$  in acetonitrile at a weight ratio of 9:1. The solution was mixed for 2 h and then cast on to a glass dish. The PEO electrolyte film was placed in a vacuum oven and heated at 50 °C for 12 h. All preparations of the polymer electrolyte were carried out in glove box-filled with argon. The ionic conductivity of the PEO electrolyte was determined from the a.c. impedance spectrum of a blocking cell that was assembled by sandwiching the PEO polymer electrolyte between two stainless-steel (SS) electrodes. The data were collected over a frequency range from 10 mHz to 100 kHz.

The Na/PEO/S battery was assembled in a stainless-steel cell holder made from a Swagelock union with polypropylene ferrules. The battery was charged and discharged at 90 °C at a constant current density of 0.144 mA cm<sup>-2</sup>. The cut-off voltages for charge and discharge were 3.0 and 1.0 V, respectively.

## 3. Results and discussion

Fig. 1 presents the X-ray diffraction pattern of the raw materials and the sulfur electrode. The X-ray diffractometer (XRD) data of elemental sulfur (a) coincides with an orthorhombic structure, which is known as a stable sulfur phase below 95.5 °C [22]. Carbon (b) shows single broad peak, which is related to a nanocrystalline structure. The two sharp peaks of PEO (c) indicate a crystalline structure [22]. The XRD pattern of the sulfur electrode (d) displays an orthorhombic sulfur phase and a crystalline PEO phase only. No traces of compounds related to sulfur, carbon or PEO are found. Thus, there are no crystal structural changes during fabrication of the sulfur electrode film, which is comprised of a mixture of sulfur, carbon, and PEO only.

Differential scanning calorimetry (DSC) curves are presented in Fig. 2. The sulfur powder (a) has two endothermic peaks, which may be related with the elemental sulfur [22]. There is no peak of carbon powder (b), which indicates thermal stability in this temperature range. The PEO powder (c) shows

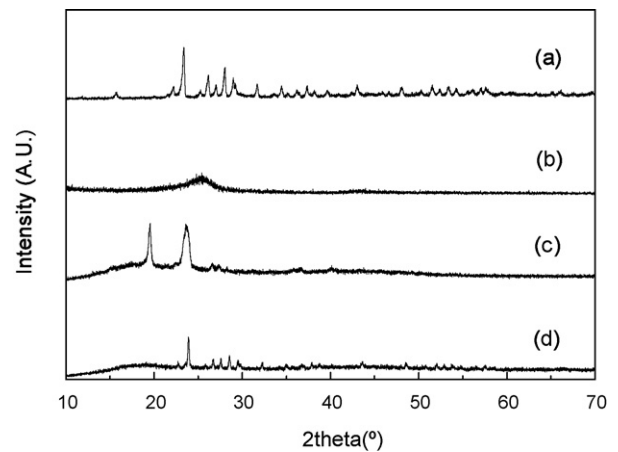


Fig. 1. XRD patterns of raw materials and sulfur electrode: (a) sulfur, (b) carbon, (c) PEO and (d) sulfur electrode.

one endothermic peak at about 68 °C, which coincides with the melting temperature of PEO [22]. For the sulfur electrode (d), three endothermic peaks are observed, which correspond to the existence of PEO and sulfur.

Scanning electron micrographs of the raw materials and the sulfur electrode are presented in Fig. 3. The shape of the sulfur powder (a) is irregular. The carbon particles (b) have a sub-micrometer diameter and the powder has a very large surface area. The sulfur electrode is distinguished by bright and dark areas. Energy dispersive spectroscopy mapping of the sulfur electrode (d) is shown in Fig. 4(b) and (c). The bright region is mostly composed of sulfur and a small amount of carbon, whereas the dark region is comprised of carbon and sulfur. Sulfur and carbon can be detected in every region of the sulfur electrode, which demonstrates uniform mixing of the components.

The a.c. impedance spectrum of the blocking cell SS/PEO/SS at 90 °C is given in Fig. 5. The high-frequency intercept on the real-axis provides the bulk resistance ( $R_b$ ) of the electrolyte. From the  $R_b$ , the specific conductivity of the polymer electrolyte is calculated to be  $3.38 \times 10^{-4}$  S cm<sup>-1</sup> at 90 °C, which is similar to a previous result reported for the PEO electrolyte [15].

The first discharge curve of the Na/PEO/S battery at 90 °C is given in Fig. 6. The first discharge curve has a high discharge

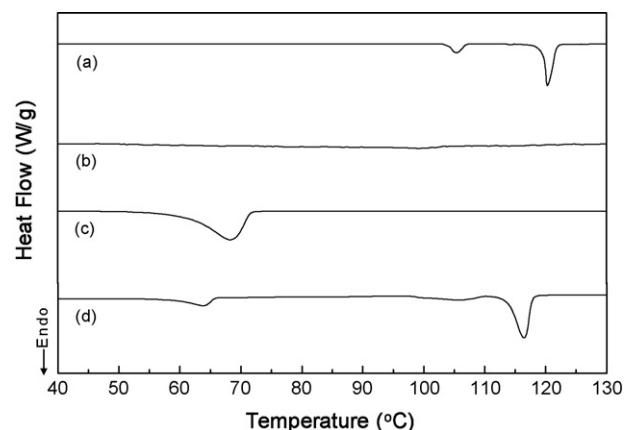


Fig. 2. Differential scanning calorimetry curves of raw materials and sulfur electrode: (a) sulfur, (b) carbon, (c) PEO and (d) sulfur electrode.

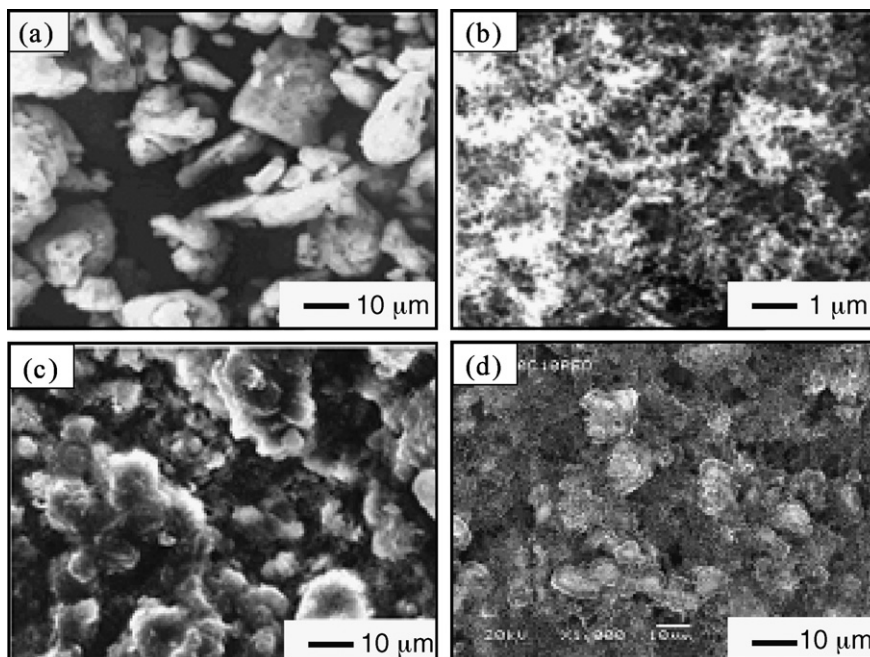
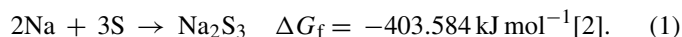


Fig. 3. Scanning electron micrographs of raw materials and sulfur electrode: (a) sulfur; (b) carbon; (c) PEO; (d) sulfur electrode.

capacity of  $505 \text{ mAh g}^{-1}$  sulfur and two potential plateaux, at 2.28 and 1.73 V, respectively, which can be related to two different reduction steps of sulfur by sodium. These results are similar to those reported for a high-temperature Na/S battery [5,6] and a Na/PVdF/S battery at room temperature [17] (PVdF=poly(vinylidene difluoride)). The phase diagram between sodium and sulfur shows several compounds such as  $\text{Na}_2\text{S}$ ,  $\text{NaS}$ ,  $\text{Na}_2\text{S}_3$ ,  $\text{NaS}_2$ ,  $\text{Na}_2\text{S}_5$  [2]. During the discharge process, elemental sulfur can be converted to sodium sulfides by

electrochemical reaction with sodium. From thermodynamic considerations, the following reactions can be proposed. The electromotive force ( $E_0$ ) of battery can be calculated from the value of the Gibbs free energy of formation ( $\Delta G_f$ ).



$$E_0 = 2.09 \text{ V.}$$

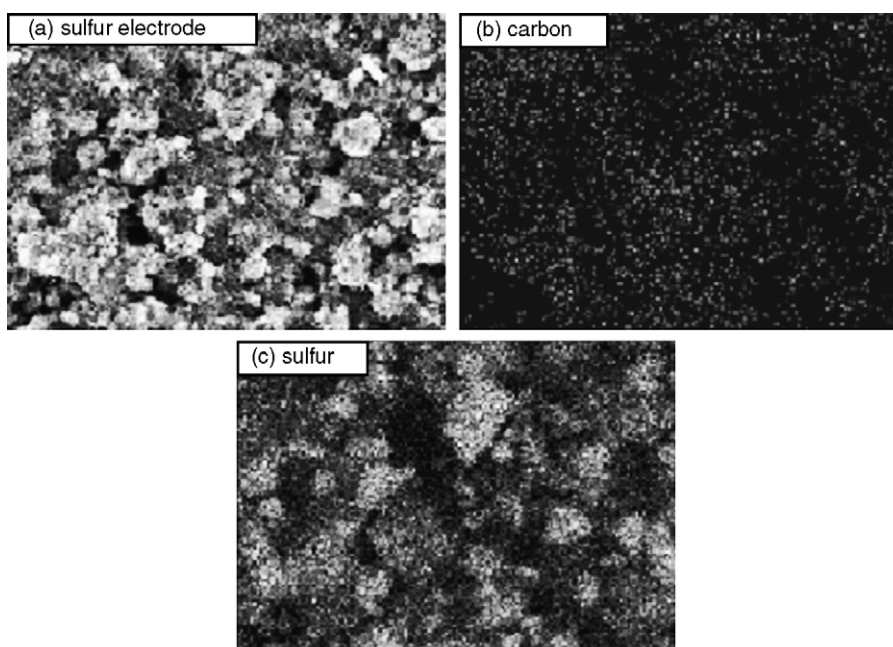
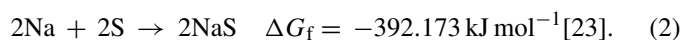


Fig. 4. Scanning electron micrographs and EDS mapping of sulfur electrode: (a) SEM image and distribution of (b) carbon and (c) sulfur.

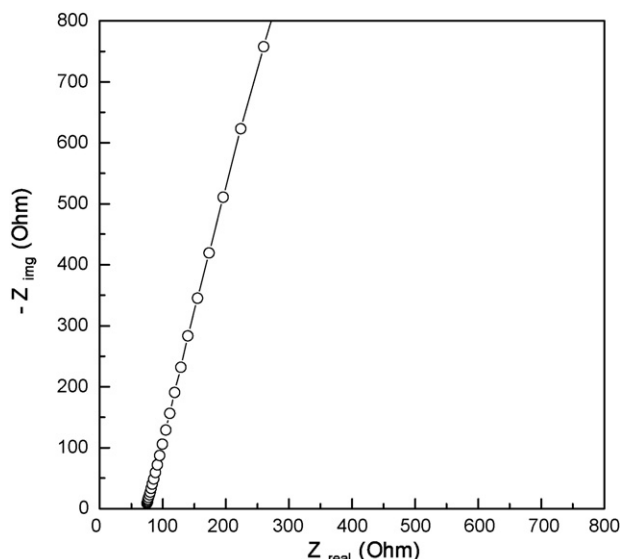
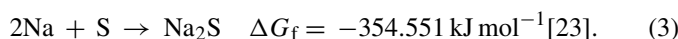


Fig. 5. A.C. impedance data of blocking cell as a complex plane plot.

$$E_0 = 2.03 \text{ V.}$$



$$E_0 = 1.84 \text{ V.}$$

The theoretical specific energy of  $\text{Na}_2\text{S}_5$ ,  $\text{Na}_2\text{S}_4$ ,  $\text{Na}_2\text{S}_3$ ,  $\text{NaS}$  and  $\text{Na}_2\text{S}$  is calculated as 335, 419, 558, 837 and 1675  $\text{mAh g}^{-1}$  sulfur, respectively. The  $E_0$  of  $\text{Na}_2\text{S}_3$ ,  $\text{NaS}$ , and  $\text{Na}_2\text{S}$  is 2.09, 2.03 and 1.84 V, respectively. Since the upper plateau potential of 2.27 V shown in Fig. 6 is higher than 2.09 V, the region cannot be explained by the formation of  $\text{NaS}$ ,  $\text{Na}_2\text{S}_3$ , or  $\text{Na}_2\text{S}$ , and therefore may be associated with high polysulfides such as  $\text{Na}_2\text{S}_4$ ,  $\text{Na}_2\text{S}_5$  ( $\text{Na}_2\text{S}_n$ ,  $n > 4$ ). The lower plateau region, 1.73 V, may originate from the formation of  $\text{Na}_2\text{S}$ ,  $\text{NaS}$  or  $\text{Na}_2\text{S}_3$  ( $\text{Na}_2\text{S}_n$ ,  $n \leq 3$ ). If all the elemental sulfur changes to  $\text{Na}_2\text{S}$ ,  $\text{NaS}$ ,  $\text{Na}_2\text{S}_3$  by Eq. (1) or (2), the first discharge capacity should be 1675, 838 or 558  $\text{mAh g}^{-1}$  sulfur, respectively. The first discharge capacity shown in Fig. 6, however, is about 505  $\text{mAh g}^{-1}$  sulfur, which is similar to that expected for the formation of  $\text{Na}_2\text{S}_n$  ( $n \leq 3$ ), especially  $\text{Na}_2\text{S}_3$ . The upper plateau region may be related to

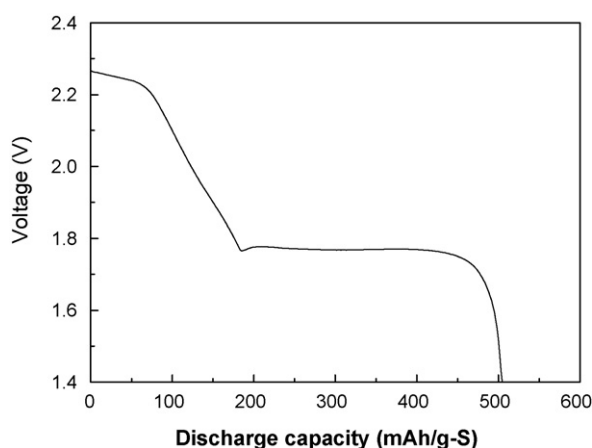


Fig. 6. First discharge curve of Na/PEO/S battery at 90 °C.

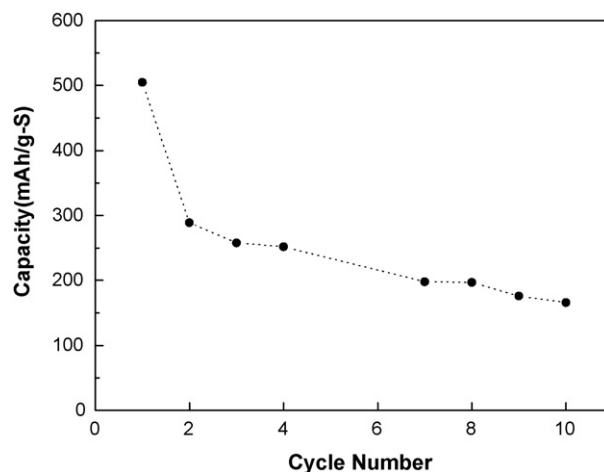


Fig. 7. Discharge capacity as a function of cycle number.

the reduction of sulfur to  $\text{Na}_2\text{S}_4$  or  $\text{Na}_2\text{S}_5$ , and lower plateau to the reduction of sulfur to  $\text{Na}_2\text{S}_n$  ( $n \leq 3$ ).

The discharge capacity of the Na/S battery as a function of cycling number is given in Fig. 7. The battery experiences a sharp decline in capacity over the next few cycles, and then the fade rate diminishes substantially. The discharge capacity remains at 166  $\text{mAh g}^{-1}$  sulfur after 10 cycles, which is higher than that given by a Na/PVdF/S battery at room temperature [17]. The severe capacity fading for a few cycles is probably related to the formation of irreversible sodium polysulfides that are not oxidized to elemental sulfur during charging.

#### 4. Conclusions

An all-solid Na/S battery using a PEO polymer electrolyte gives a high initial discharge capacity of 505  $\text{mAh g}^{-1}$  sulfur at 90 °C with plateau potential regions at 2.28 and 1.73 V. From thermodynamic considerations, the lower plateau region should originate from the formation of  $\text{Na}_2\text{S}$ ,  $\text{Na}_2\text{S}_2$ ,  $\text{Na}_2\text{S}_3$  and upper plateau region from  $\text{Na}_2\text{S}_4$  and  $\text{Na}_2\text{S}_5$ . The discharge capacity decreases continuously during repeated charge-discharge cycling, but remains at 166  $\text{mAh g}^{-1}$  sulfur after 10 cycles, which is higher than for a Na/PVdF/S battery at room temperature. The PEO electrolyte with  $\text{NaCF}_3\text{SO}_3$  salt has a sodium ion conductivity of  $3.38 \times 10^{-4} \text{ S cm}^{-1}$  at 90 °C. It is possible to fabricate an all-solid Na/S battery at 90 °C, but its cycling property has to be improved for practical applications.

#### Acknowledgements

This work was supported by University IT Research Center Project from Ministry of Information and Communication Republic Korea.

#### References

- [1] R. Janot, D. Guérard, Prog. Mater. Sci. 50 (2005) 1.
- [2] J.L. Sudworth, A.R. Tilley, The Sodium Sulfur Battery, Chapman & Hall, New York, 1985.

- [3] J.H. Shin, S.S. Jung, K.W. Kim, H.J. Ahn, J.H. Ahn, *J. Mater. Sci.: Mater. Electron.* 13 (2002) 727.
- [4] L.A. Montoro, J.M. Rosolen, J.H. Shin, S. Passerini, *Electrochim. Acta* 49 (2004) 3419.
- [5] R. Okuyama, E. Nomura, *J. Power Sources* 77 (1999) 164.
- [6] J.T. Kummer, N. Weber, *SAE Trans.* 76 (1968) 1003.
- [7] N.S. Choudhury, *J. Electrochem. Soc.* 133 (1986) 429.
- [8] M.C.H. McKubre, F.L. Tanzella, S.I. Smedley, *J. Electrochem. Soc.* 136 (1989) 1962.
- [9] H. Tokoi, K. Takahashi, S. Shimoyashiki, *J. Electrochem. Soc.* 139 (1992) 10.
- [10] N. Terada, T. Yanagi, S. Arai, M. Yoshikawa, K. Ohta, N. Nakajima, A. Yanai, N. Arai, *J. Power Sources* 100 (2001) 80.
- [11] J.M. Tarascon, A.S. Gozdz, C. Schmutz, F. Shokoohi, P.C. Warren, *Solid State Ionics* 86–88 (1996) 49.
- [12] J. Castillo, I. Delgado, M. Chacón, R.A. Vargas, *Electrochim. Acta* 46 (2001) 1695.
- [13] T. Srekanth, M.J. Reddy, S. Ramalingaiah, U.V. Subba Rao, *J. Power Sources* 79 (1999) 105.
- [14] C.P. Rhodes, R. Frech, *Solid State Ionics* 121 (1999) 91.
- [15] S.J. Pai, Y.C. Bae, Y.K. Sun, *J. Electrochem. Soc.* 152 (2005) A864.
- [16] S.A. Hashmi, A. Kumar, S.K. Tripathi, *Eur. Polym. J.* 41 (2005) 1373.
- [17] C.W. Park, J.H. Ahn, H.S. Ryu, K.W. Kim, H.J. Ahn, *Electrochem. Solid-State Lett.* 9 (1997) A123.
- [18] J.H. Shin, Y.T. Lim, K.W. Kim, H.J. Ahn, J.H. Ahn, *J. Power Sources* 107 (2002) 103.
- [19] D. Marmorstein, T.H. Yu, K.A. Striebel, F.R. McLarnon, J. Hou, E.J. Cairns, *J. Power Sources* 89 (2000) 219.
- [20] H.S. Ryu, H.J. Ahn, K.W. Kim, J.H. Ahn, J.Y. Lee, *J. Power Sources* 153 (2006) 360.
- [21] K.M. Abraham, Z. Jiang, *J. Electrochem. Soc.* 144 (1997) L136.
- [22] C.W. Park, H.S. Ryu, K.W. Kim, B.Y. Hur, K.K. Cho, J.H. Ahn, J.Y. Lee, H.J. Ahn, *Met. Mater. Int.* 10 (2004) 375.
- [23] M.W. Chase, C.A. Davies, J.R. Downey, D.J. Frurip, R.A. McDonald, A.N. Syverud, *JANAF Thermochemical Tables*, third ed., American Institute of Physics, 1986.